IOPscience iopscience.iop.org

Home Search Collections Journals About Contact us My IOPscience

A systematic study of electronic states in n-$Al_xGa_{1-x}As$/GaAs/n-$Al_xGa_{1-x}As$ selectively doped double-heterojunction structures

This article has been downloaded from IOPscience. Please scroll down to see the full text article.

1993 J. Phys.: Condens. Matter 5 6437

(http://iopscience.iop.org/0953-8984/5/35/009)

View the table of contents for this issue, or go to the journal homepage for more

Download details:
IP Address: 171.66.16.159
The article was downloaded on 12/05/2010 at 14:23

Please note that terms and conditions apply.

J. Phys.: Condens. Matter 5 (1993) 6437–6446. Printed in the UK

A systematic study of electronic states in n-$Al_xGa_{1-x}As$/ $GaAs$/n-$Al_xGa_{1-x}As$ selectively doped double-heterojunction structures

C D Simserides and G P Triberis

Department of Physics, Solid State Section, University of Athens, Panepistimiopolis, 157 84 Zografos, Athens, Greece

Received 30 March 1993, in final form 27 May 1993

Abstract. The electron concentration, the wavefunctions and the energy levels of a n-$Al_xGa_{1-x}As$/GaAs/n-$Al_xGa_{1-x}As$ double heterojunction are evaluated by solving Schrödinger and Poisson equations self-consistently. We investigate, at zero temperature, the dependence of the sheet electron concentration, and the subband populations on the well width, spacer thickness and doping concentration, for Al mole fraction $x = 0.3$. We give physical interpretations of some interesting characteristics observed. The transition from a 'perfect' square well to a system of 'two separated heterojunctions' is systematically studied. Our results are in excellent agreement with previous experiments.

1. Introduction

The quasi two-dimensional electron gas (Q2DEG) which accumulates at the GaAs side of a n-$Al_xGa_{1-x}As$/GaAs selectively-doped single heterojunction (SD-SH) exhibits high electron mobilities, especially at low temperatures (Dingle *et al* 1978, Hiyamizu *et al* 1983, Hirakawa *et al* 1986). However, for the sheet electron concentration, N_s, which also plays a fundamental role in determining the channel conductivity, a maximum obtainable value has been found to exist, which depends on the structural parameters of the heterojunction (not larger than 1×10^{12} cm^{-2}) (Hirakawa *et al* 1984). An alternative and more effective approach to achieve higher N_s than such a limit, is to use a selectively-doped double heterojunction (SD-DH) (Hamaguchi *et al* 1984, Inoue *et al* 1984, Inoue and Sakaki 1984, Inoue *et al* 1985a, Miyatsuji *et al* 1985, Burkhard *et al* 1986, Inoue *et al* 1986). Studies of rectangular wells formed in an $Al_xGa_{1-x}As$/GaAs/$Al_xGa_{1-x}As$ structure start to appear in the early seventies (Dingle *et al* 1974). Although there has been a lot of discussion about the 'inverted interface problem' (Morcoç *et al* 1981, Sasa *et al* 1984, Sasa *et al* 1985), a number of authors have reported that this problem can be overcome in several ways (Drummond *et al* 1983, Inoue *et al* 1984, Inoue and Sakaki 1984, Inoue *et al* 1985b). This was the motivation for the present systematic study of such a system.

Several theoretical methods have been presented in the literature (variational etc), but the most reliable among them are the self-consistent calculations for heterojunctions (Ando 1982a, Ando 1982b, Stern and Das Sarma 1984, Hihara and Hamaguchi 1985, Hurkx and van Haeringen 1985) and SD-DH (Hamaguchi *et al* 1984, Inoue *et al* 1984, Inoue and Sakaki 1984, Inoue *et al* 1985a, Miyatsuji *et al* 1985, Roan and Chuang 1991). In the case of SD-DH, in recent years, although a number of theoretical studies have been presented, there is a lack of a systematic study, concerning all the parameters involved, bridging the

0953-8984/93/356437+10$07.50 © 1993 IOP Publishing Ltd

heterojunctions with the SD-DH structures, and giving a consistent physical interpretation of the results. In the present work we attempt a contribution in this direction. In section 2 we give a description of the SD-DH system, in section 3 the basic theoretical background is presented together with the algorithm used to solve simultaneously, within the effective mass approximation, Schrödinger and Poisson equations. In section 4 the results of the calculations at $T = 0$ K are shown and discussed together with comparisons with theoretical and experimental results of other workers.

2. Description of the system

In figure 1(a) a schematic energy diagram of the valence and the conduction band of a n-$Al_xGa_{1-x}As$/GaAs/n-$Al_xGa_{1-x}As$ system (the SD-DH structure) is presented for the case in which the materials are considered to be separated. The GaAs well width is $2L$. The $Al_xGa_{1-x}As$ layers, which have finite length, are uniformly doped with donors of concentration N_d, except from the two spacer layers of width D_s, from both sides of the GaAs well. The donor levels are all supposed to lie at an energy ΔE_d below the bottom of the $Al_xGa_{1-x}As$ conduction band. All layers have a small unintentional acceptor doping N_a. The acceptor levels are supposed to lie at an energy ΔE_a above the top of the valence band, although the exact value of ΔE_a is of no interest here. $\Delta E_c = U_0$, and ΔE_v are the conduction and the valence band offsets, respectively. The layers, considered separated above, are joined to form the heterostructure.

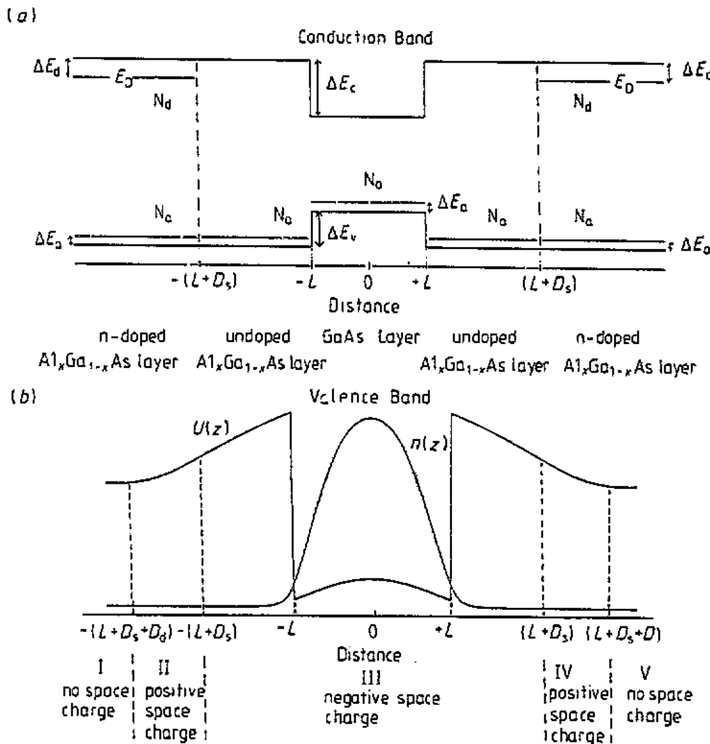

Figure 1. Schematic energy diagrams of a SD-DH structure. (a) the materials are considered to be separated. (b) the conduction band of the SD-DH structure, showing the band bending, the various space charge regions, and $n(z)$.

Electrons are moving from the higher lying donor energy levels to the lower lying conduction band and acceptor levels of GaAs. This redistribution of carriers results in the formation of (i) region III which consists of the spacers and the GaAs layer with negative

space charge due to ionized acceptors, (ii) regions II and IV, each of width D_d, with positive space charge due to ionized donors ($N_a \ll N_d$) and (iii) regions I, V where there is no space charge. The electrons are mainly distributed in the well and their concentration, $n(z)$, which depends only on the coordinate z perpendicular to the interfaces, decays into the barriers, being zero at regions I and V. The qualitative diagram of the conduction band is given in figure 1(b).

This redistribution of charges causes, together with the potential energy discontinuities and the exchange–correlation potential energy, U_{xc}, what is known as 'band bending'. This is also shown in figure 1(b).

The charge density is given by

$$\rho(z) = \begin{cases} -en(z) & \text{region I: } z \leqslant -[D_d + D_s + L] \\ e[N_d - N_a - n(z)] & \text{region II: } -[D_d + D_s + L] < z \leqslant -[D_s + L] \\ -e[N_a + n(z)] & \text{region, III: } -[D_s + L] < z \leqslant [D_s + L] \\ e[N_d - N_a - n(z)] & \text{region IV: } [D_s + L] < z \leqslant [D_d + D_s + L] \\ -en(z) & \text{region V: } z > [D_d + D_s + L]. \end{cases} \tag{2.1}$$

For realistic values of N_d, all the GaAs layer and spacers are completely depleted. $n(z)$ in regions I, V, as we have already stated, is zero.

The total potential energy is

$$U(z) = U_c(z) + U_{\text{band offset}} + U_{xc}(z) \tag{2.2}$$

whre $U_c(z)$ is the Coulomb potential energy, obtained from the solution of the Poisson equation

$$d^2U_c(z)/dz^2 = e\rho(z)/\epsilon_0\epsilon \tag{2.3}$$

where, $-e$ is the electron charge, ϵ_0 and ϵ, are the vacuum and the relative dielectric constants, respectively. $U_{\text{band offset}}$ is U_0 for the $Al_xGa_{1-x}As$ layers and zero for the GaAs layer i.e. it is the potential energy discontinuity term. The formation of interfaces retains constant the band offsets as long as (i) interfaces are abrupt (ii) band offsets and electron affinities are independent of N_d and N_a, and (iii) no surface charges or dipoles are formed (Heime 1989). For U_{xc} we adopt the expression given by Hurkx and van Haeringen (1985)

$$U_{xc}(z) = -0.0783(e^2/\epsilon_0\epsilon)[n(z)]^{1/3} \tag{2.4}$$

which is the dominant term (over 90%) in the full expression given by Stern and Das Sarma (1984). $U_{xc}(z)$ is not neglected because it has a small but not negligible influence on the sheet electron concentration (Ando 1982a). According to our calculations, this is 4–5%. We ignore the image potential energy term (Stern and Das Sarma 1984), because the difference in the dielectric constants of $Al_{0.3}Ga_{0.7}As$ and GaAs is very small. The exact potential energy depends on the specific electron gas distribution. The electron distribution reshapes the well, while it, itself, is reshaped by the shape of the well.

3. Theoretical calculations

The above discussion imposes the necessity of simultaneous solution of Schrödinger and Poisson equations. Starting from the Schrödinger equation, applying the effective mass approximation (Slater 1949), taking into account the fact that the $Al_xGa_{1-x}As$ effective mass is different from the GaAs effective mass one should use the BenDaniel–Duke equation (BenDaniel and Duke 1966). However, the penetration of the envelope function into the

$Al_xGa_{1-x}As$ layers turns out to be small, and consequently we can use the value of GaAs effective mass, m^*, throughout our system. This assumption results in a Schrödinger-like equation, where variables can be separated.

The electron density at $T = 0$ K (postulating $E_F \equiv 0$) is

$$n(z) = -\sum_{i,\text{occupied}} \frac{m^* E_i}{\pi \hbar^2} |\zeta_i(z)|^2 \tag{3.1}$$

where $\zeta_i(z)$ is the z-axis envelope function with corresponding eigenvalues E_i.

It is now necessary to determine the asymptotic behaviour of the potential energy $U(z)$ in the bulk material, away from the well i.e. in the regions I and V, and impose the boundary conditions for the envelope functions. At $T = 0$ K, E_F can be chosen as the highest populated level. Clearly, this is the donor level E_D; thus, $E_F = E_D$. Then, the energy distance between the Fermi level and the bottom of the conduction band is ΔE_d. We have already postulated $E_F \equiv 0$. Therefore the asymptotic values of the potential energy are

$$U(\text{bulk}) = \Delta E_d. \tag{3.2}$$

On the other hand, $\zeta_i(z)$ decay exponentially in regions I and V.

The algorithm used to solve simultaneously the envelope function equation and the Poisson equation consists of the following steps:

(i) Start with an initial guess of the potential energy U_{in} (for example the band offsets' potential energy) and solve the one-dimensional Schrödinger-like z-axis envelope function equation. In this way, we obtain E_i and $\zeta_i(z)$.

(ii) Calculate $n(z)$ from (3.1).

(iii) The charge conservation equation gives

$$D_d = [N_s + 2(L + D_s)N_a]/2(N_d - N_a) \tag{3.3}$$

where the sheet electron density is

$$N_s = \int_{\text{bulk }(I)}^{\text{bulk }(V)} n(z)\,\mathrm{d}z. \tag{3.4}$$

(iv) Calculate $\rho(z)$ from (2.1).

(v) Obtain $U_c(z)$ solving (2.3). In other words integrate $\rho(z)$ twice, starting from distant parts of the left and right sides of the $Al_xGa_{1-x}As$ layers (the bulk material), where there is no charge. D_d is usually much smaller than 100 Å. In our calculations its largest value does not exceed 600 Å, thus, the boundary conditions for the Coulomb potential energy and its derivative are imposed at finite distance from each spacer. At bulk $Al_xGa_{1-x}As$, $U_{xc}(\text{bulk}) = 0$, $U(\text{bulk}) = \Delta E_d$. Thus,

$$U_c(\text{bulk}) = \Delta E_d - U_0. \tag{3.5}$$

Also, in bulk $Al_xGa_{1-x}As$

$$(\mathrm{d}U_c/\mathrm{d}z)(\text{bulk}) = 0. \tag{3.6}$$

(vi) Calculate $U_{xc}(z)$ from (2.4).

(vii) Calculate $U_{out} = U(z)$ from (2.2).

(viii) Is U_{out} 'very close to' U_{in}? If not:

(ix) use Tchebycheff iteration scheme (Akai and Dederichs 1985) to calculate new U_{in}, and so on, until the desired accuracy is succeeded.

4. Results

To start with it is necessary to make some remarks concerning the values of the basic parameters involved in our calculations.

The determination of ΔE_c and ΔE_v is not a completely solved problem yet (Miller *et al* 1985, Heime 1989, van Vechten and Malloy 1990, Krijn 1991). However, for Al mole fraction $x = 0.3$, which is the case here, the value we use, $\Delta E_c = 300$ meV is widely adopted (Inoue *et al* 1984, Hurkx and van Haeringen 1985). Furthermore, we use $\Delta E_d = 96$ meV which is the experimental value for this Al mole fraction (Ishibashi *et al* 1982, Watanabe and Maeda 1984). Here it should be noticed that this is a 'mean' value averaging the shallow and Dx donors activation energies for this Al mole fraction (Ishikawa *et al* 1982, Ishibashi *et al* 1982, Watanabe and Maeda 1984, Watanabe *et al* 1984, Mizuta *et al* 1985). The correct value of ΔE_d has not always been used in theoretical calculations, although it is of great importance. For example, Hurkx and van Haeringen (1985), for $x = 0.3$, use $\Delta E_d = 50$ meV, instead of the correct value 96 meV; Cho *et al* (1987), for $x = 0.33$, use $\Delta E_d = 50$ meV, instead of the correct value 125 meV. These authors using smaller value of ΔE_d overestimate the sheet electron concentration. In section 4.1, for both $Al_{0.3}Ga_{0.7}As$ and GaAs, for simplicity, we use the value of $Al_{0.3}Ga_{0.7}As$ dielectric constant i.e. 12.244. This results in a slight overestimation of N_s (0.5–1%). In the rest of the calculations we use the exact values of the $Al_{0.3}Ga_{0.7}As$ and GaAs dielectric constants i.e. 12.244 and 13.18, respectively. We obtained these values by interpolating AlAs and GaAs dielectric constants (Jaros 1989). In our calculations, for simplicity we use $m^* = 0.067m_e$ i.e. its value for GaAs. This value is smaller than the one that should be used taking into account the small penetration of the envelope functions into the $Al_{0.3}Ga_{0.7}As$ layers (Ando 1982a, Ando and Mori 1982). It has been reported (Hiyamizu *et al* 1983, Mendez *et al* 1984) that the sheet electron concentration remains constant as a function of temperature up to 100 K. This allows us to compare our theoretical results with experiments performed at 4.2 K and 77 K.

4.1. From 'the perfect square well' to 'the double heterojunction'

In figure 2 the sheet electron concentration N_s, and the subband populations N_i as a function of the well width $2L$ are presented. Figure 3 shows N_s, the subband energies E_0 to E_3, and the energy of the centre of the bottom of the well E_{bot}, as a function of the well width $2L$.

From (3.1) we obtain

$$N_s = -\sum_{i,\text{occupied}} \frac{m^* E_i}{\pi\hbar^2} \sum_{i,\text{occupied}} N_i \tag{4.1}$$

where N_i is the ith occupied subband population. In a 'perfect square well' the well width increase leads to a lowering of the energy levels (Bastard 1988). Consequently, increasing $2L$, N_s increases. However, when E_0, the lower subband energy level, touches the bottom of the well a qualitative change begins: the transition from 'the square well' to a system of 'two separated heterojunctions'. As the well becomes wider E_0 increases, while E_1 continues to fall, and when both E_0 and E_1 are below the bottom of the conduction band in the centre of the well, they can be described as the result of the splitting of the 'two heterojunctions' ground states. If the well width continues to increase the 'two heterojunctions' distance increases. The larger is the separation of the 'two heterojunctions' the smaller is the splitting. So, according to our calculations while in a 300 Å well, energy separation between E_0 and E_1 is 5.5 meV, in a 600 Å well this energy difference has diminished to 0.03 meV. The mean value of E_0 and E_1, which almost exclusively determines N_s remains almost constant

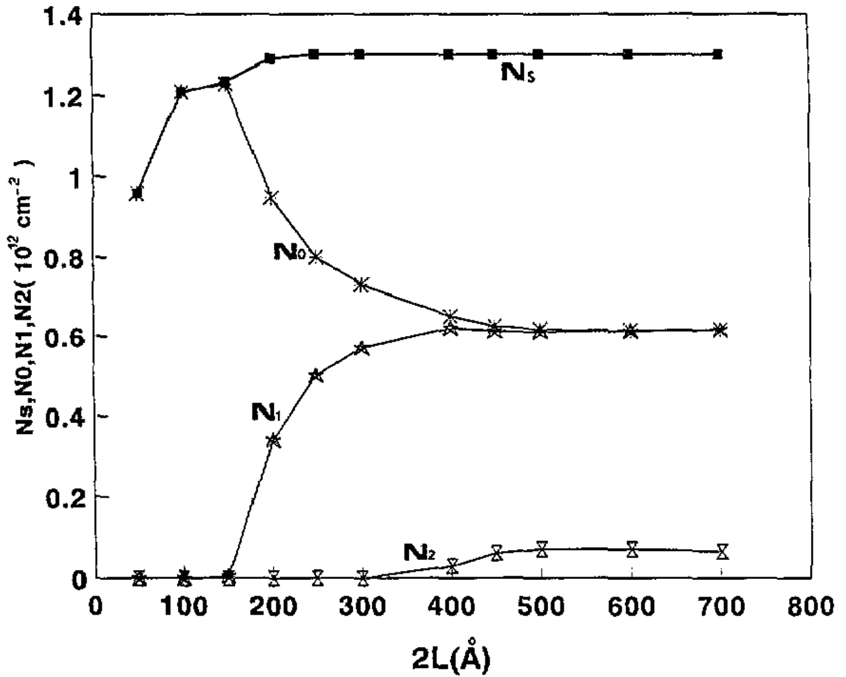

Figure 2. The sheet electron concentration N_s, and the subband populations N_i as a function of the well width; $N_d = 1 \times 10^{18}$ cm^{-3}, $D_s = 100$ Å, and $N_a = 5 \times 10^{14}$ cm^{-3}.

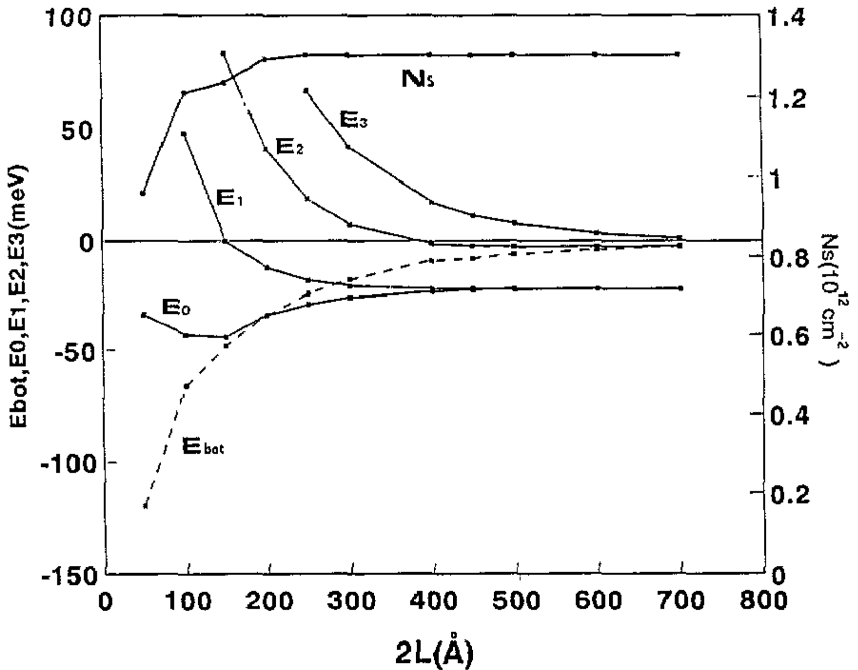

Figure 3. The sheet electron concentration N_s, the subband energies E_i $(i = 0, 1, 2, 3)$, and E_{bot} as a function of the well width; $N_d = 1 \times 10^{18}$ cm^{-3}, $D_s = 100$ Å, and $N_a = 5 \times 10^{14}$ cm^{-3}.

(1.3×10^{12} cm^{-2}) for $2L > 250$ Å. Consequently N_s saturates, taking twice the value of the corresponding quantity of the single heterojunction. The subband population N_2 still belongs to the double heterojunction structure. E_2 and E_3 can also be seen as the result of the splitting of the first excited states of the two separated heterojunctions. Thus, while for $2L = 250$ Å energy separation between E_2 and E_3 is 48 meV, in a 600 Å well this energy difference has diminished to 6 meV. For $2L = 700$ Å, the energy difference between E_2 and E_3 decreases much more to 3.6 meV. We can now look at our system as a system of 'two separate heterojunctions'. Figures 2 and 3 give a full description of the above-mentioned transition.

The value of N_s is the same as the one measured and calculated by Inoue *et al* (1984) and Inoue *et al* (1985a), for $2L = 300$ Å. Also the energy levels, as we can conclude from the figure they present, are in agreement with our calculations. A saturation in a one-side doped square well has been presented, without any explanation, by Cho *et al* (1987). In that case, increasing the well width, a single heterojunction's limit is reached.

Our results are also confirmed by Sasa *et al* (1985) who measured the N_s and N_i dependence of a SD-DH structure on the well width in the range of 60 Å–1000 Å, for Al mole fraction $x = 0.28$ and $N_d = 1 \times 10^{18}$ cm^{-3}. Due to unintentional asymmetric Si-doping, on only one side of their well is D_s different from zero, thus, the ground states of the two 'separated heterojunctions' (the large well-width limit) do not coincide; consequently N_0 and N_1, do not coincide either. The saturation effects and the form of the N_s and N_i dependence observed are similar to our results. In their structure, electrons start to populate the first subband for $2L > 130$ Å, while in our symmetrically doped structure, for $2L > 150$ Å. However, they do not give any physical explanation for the observed behaviour or any calculational details as far as their theoretical results are concerned.

4.2. Doping dependence

In figure 4 the sheet electron concentration N_s, together with the subband populations N_i, and the depletion length D_d are presented as a function of the doping concentration N_d, for $2L = 150$ Å $N_a = 5 \times 10^{14}$ cm^{-3} and $D_s = 100$ Å. Electrons start to populate the first excited subband only for $N_d > 1 \times 10^{18}$ cm^{-3}. A characteristic saturation of N_s (1.4×10^{12} cm^{-2}) is observed. The same behaviour is also observed for the other values of the well width.

From (3.3) it follows

$$N_s = 2D_d(N_d - N_a) - 2(L + D_s)N_a = N_s(N_d, D_d) \tag{4.2}$$

because we keep L, D_s and N_a constants. Thus,

$$\mathrm{d}(N_s) = (\partial N_s/\partial N_d)\,\mathrm{d}(N_d) + (\partial N_s/\partial D_d)\,\mathrm{d}(D_d) \tag{4.3}$$

or

$$\mathrm{d}(N_s) = 2D_d\mathrm{d}(N_d) + 2(N_d - N_a)\,\mathrm{d}(D_d). \tag{4.4}$$

Here we have two opposite mechanisms: (i) taking D_d = constant, it follows that $\partial N_s/\partial N_d > 0$. (ii) taking N_d = constant it follows that $\partial N_s/\partial D_d > 0$. However, an increase of N_d results in a decrease of D_d, i.e. if $\mathrm{d}(N_d) > 0$, then $\mathrm{d}(D_d) < 0$. Thus, the first term in the RHS of (4.3) or (4.4) is positive, but decreases in absolute value as N_d increases, while the second term in the RHS of (4.3) or (4.4) is negative and also decreases in absolute value as N_d increases. From our calculations it follows that for small values of N_d, the first term is larger than the second one in absolute value, so with increasing N_d, N_s increases.

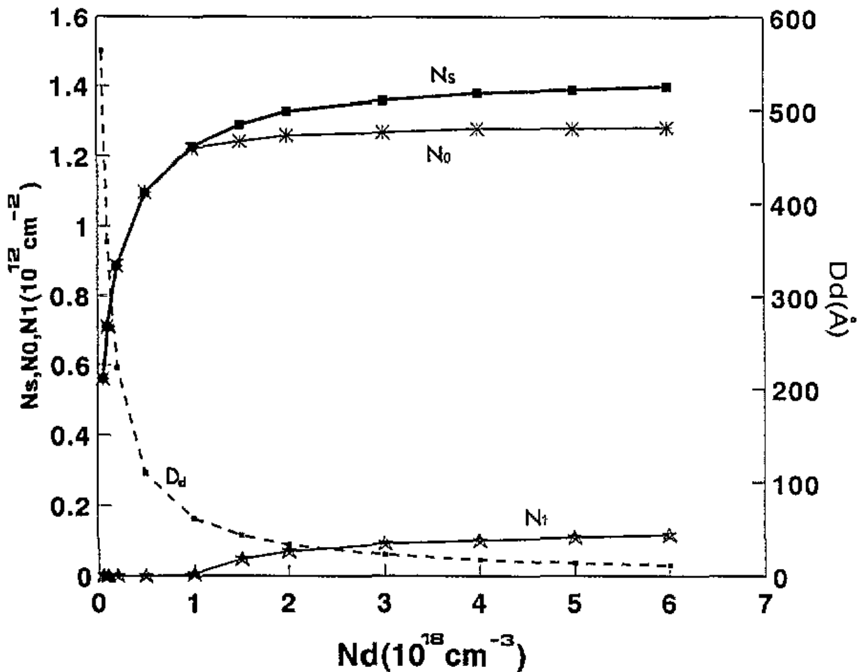

Figure 4. The sheet electron concentration N_s, the subband populations N_i, and the depletion length D_d, as a function of the doping concentration N_d, for a characteristic value of the well width $2L = 150$ Å; $D_s = 100$ Å, and $N_a = 5 \times 10^{14}$ cm^{-3}. Electrons populate the first excited subband only for $N_d > 1 \times 10^{18}$ cm^{-3}.

However, as we increase N_d, the absolute value of the first term falls faster and finally one cancels the other i.e. saturation occurs.

The charge conservation equation is enriched in the case of single heterojunctions, where the acceptors' depletion length must be taken into account, resulting in additional mechanisms. Following the same philosophy the $N_s = N_s(N_d)$ behaviour presented by Hurkx and van Haeringen (1985), although they assume an 'infinite' GaAs layer, can be explained. On the other hand, when acceptors are not taken into account, although this is not a realistic assumption for single heterojunctions, following the same lines saturation will occur (Hihara and Hamaguchi 1985). Saturation will occur when the GaAs layer, which of course is not infinite, is all depeleted. These, together with the $N_s = N_s(D_s)$ behaviour for these systems, will be analytically presented in the near future.

According to our calculations, variation of N_a from 0.1×10^{14} cm^{-3} to 100×10^{14} cm^{-3} has a negligible influence on sheet electron concentration.

4.3. Spacer dependence

In figure 5 the sheet electron concentration N_s, together with the subband populations N_i, and the depletion length D_d are presented, as a function of the spacer thickness D_s, for $2L = 300$ Å; $N_d = 1 \times 10^{18}$ cm^{-3} and $N_a = 5 \times 10^{14}$ cm^{-3}. Electrons start to populate the second excited subband for $D_s < 25$ Å. A continuous fall is observed. The same behaviour is also observed for the other values of the well width.

From (3.3) it follows

$$N_s = 2D_d(N_d - N_a) - 2(L + D_s)N_a = N_s(D_s, D_d) \tag{4.5}$$

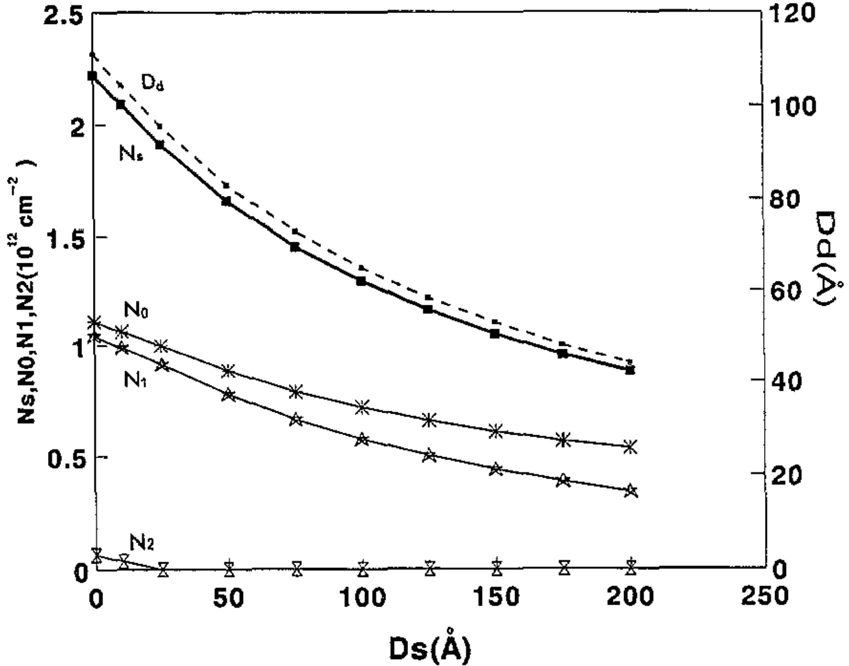

Figure 5. The sheet electron concentration N_s, the subband populations N_i and the depletion length D_d, as a function of the spacer D_s, for the characteristic value of the well width $2L = 300$ Å, $N_d = 1 \times 10^{18}$ cm^{-3}, and $N_a = 5 \times 10^{14}$ cm^{-3}. Electrons populate the second excited subband only for $D_s < 25$ Å.

because we now keep L, N_d, and N_a constants. Thus,

$$d(N_s) = (\partial N_s/\partial D_s)\,d(D_s) + (\partial N_s/\partial D_d)\,d(D_d) \tag{4.6}$$

or

$$d(N_s) = -2N_a\,d(D_s) + 2(N_d - N_a)\,d(D_d). \tag{4.7}$$

Here we have two collaborating mechanisms: (i) taking D_d = constant, it follows that $\partial N_s/\partial D_s < 0$, (ii) taking D_s = constant, it follows that $\partial N_s/\partial D_d > 0$. Here, with increasing D_s, D_d decreases; thus, if $d(D_s) > 0$ then $d(D_d) < 0$ and in the RHS of (4.6) or (4.7) both terms are negative. That is why we observe a continuous fall.

Experimental results, for $2L = 300$ Å, have been presented by Inoue *et al* (1984). Their measured values for N_s as a function of the spacer width, are in complete agreement with our theoretical results, with the exception of the experimental point $N_d = 0.4 \times 10^{18}$ cm^{-3} and D_s = 300 Å. A similar behaviour has been experimentally observed in single heterojunctions (Hirakawa *et al* 1984), and theoretically calculated for a one-side doped square well by Cho *et al* (1987). Explanation for such $N_s = N_s(D_s)$ behaviour can be interpreted following the arguments used above, taking into account in the case of single heterojunctions the existence of depletion length for acceptors.

4.4. N_s enhancement

In the structure under study two factors control the magnitude of N_s. The variation of the doping concentration N_d, and that of the spacer thickness D_s. $N_s = N_s(N_d, D_s)$ is a

2D surface. Starting from any point on this surface, one may move in two perpendicular directions, corresponding to constant N_d or D_s. In the N_d direction saturation occurs, while in the D_s direction a continuous increase of N_s is observed as we decrease D_s to zero.

Acknowledgments

The authors would like to thank Assistant Professors G Papaioannou and N Stefanou for useful discussions, and Dr A Al Zoudi for his assistance. Special thanks to Dr V Karavolas for stimulating discussions and remarks, and Mrs A Tsalpatourou for her precious assistance. The hospitality of the Nuclear Physics and Elementary Particles Section of the University of Athens is gratefully acknowledged.

References

Akai H and Dederichs P H 1985 *J. Phys. C: Solid State Phys.* **18** 2455
Ando T 1982a *J. Phys. Soc. Japan* **51** 3893
—— 1982b *J. Phys. Soc. Japan* **51** 3900
Ando T and Mori S 1982 *Surf. Sci.* **113** 124
Bastard G 1988 *Wave Mechanics Applied to Semiconductors Heterostructures* (Paris: Les Éditions de Physique)
BenDaniel D J and Duke C B 1966 *Phys. Rev.* **152** 683
Burkhard H, Schlapp W and Weimann G 1986 *Surf. Sci.* **174** 387
Cho N M, Ogale S B and Madhukar A 1987 *Phys. Rev.* B **36** 6472
Dingle R, Stormer H L, Gossard A C and Wiegmann W 1978 *Appl. Phys. Lett.* **33** 665
Dingle R, Wiegmann W and Henry C H 1974 *Phys. Rev. Lett.* **33** 827
Drummond T J, Klem J, Arnold D, Fischer R, Thorne R E, Lyons W G and Morcoç H 1983 *Appl. Phys. Lett.* **42** 615
Hamaguchi C, Miyatsuji K and Hihara H 1984 *Japan. J. Appl. Phys.* **23** L132
Heime K 1989 *In Ga As Field-Effect Transistors* (Exeter: Research Studies Press Ltd and Wiley)
Hihara H and Hamaguchi C 1985 *Solid State Commun.* **54** 485
Hirakawa K, Sakaki H and Yoshino J 1984 *Appl. Phys. Lett.* **45** 253
—— 1986 *Surf. Sci.* **170** 440
Hiyamizu S, Saito J, Nanbu K and Ishikawa T 1983 *Japan. J. Appl. Phys.* **22** L609
Hurkx G A M and van Haeringen W 1985 *J. Phys. C: Solid State Phys.* **18** 5617
Inoue K and Sakaki H 1984 *Japan. J. Appl. Phys.* **23** L61
Inoue K, Sakaki H and Yoshino J 1984 *Japan. J. Appl. Phys.* **23** L767
Inoue K, Sakaki H, Yoshino J and Hotta T 1985a *J. Appl. Phys.* **58** 4277
Inoue K, Sakaki H, Yoshino J and Yoshioka Y 1985b *Appl. Phys. Lett.* **46** 973
Inoue K, Sakaki H, Yoshino J and Hirakawa K 1986 *Surf. Sci.* **174** 382
Ishibashi T, Tarucha S and Okamoto H 1982 *Japan. J. Appl. Phys.* **21** L476
Ishikawa T, Saito J, Sasa S and Hiyamizu S 1982 *Japan. J. Appl. Phys.* **21** L675
Jaros M 1989 *Physics and Applications of Semiconductor Microstructures* (Oxford: Clarendon)
Krijn P M C M 1991 *Semicond. Sci. Technol.* **6** 27
Mendez E E, Price P J and Heiblum M 1984 *Appl. Phys. Lett.* **45** 294
Miller D A B, Chemla D S, Damen T C, Gossard A C, Wiegmann W, Wood T H and Burrus C A 1985 *Phys. Rev.* B **32** 1043
Miyatsuji K, Hihara H and Hamaguchi C 1985 *Superlatt. Microstruct.* **1** 43
Mizuta M, Tachikawa M, Kukimoto H and Minomura S 1985 *Japan. J. Appl. Phys.* **24** L143
Morcoç H, Drummond T J, Thorne R E and Kopp W 1981 *Japan. J. Appl. Phys.* **20** L913
Roan E J and Chuang S L 1991 *J. Appl. Phys.* **69** 3249
Sasa S, Saito J, Nanbu K, Ishikawa T and Hiyamizu S 1984 *Japan. J. Appl. Phys.* **23** L573
Sasa S, Saito J, Nanbu K, Ishikawa T, Hiyamizu S and Inoue M 1985 *Japan. J. Appl. Phys.* **24** L281
Slater J C 1949 *Phys. Rev.* **76** 1592
Stern F and Das Sarma S 1984 *Phys. Rev.* B **30** 840
van Vechten J A and Malloy K J 1990 *J. Phys.: Condens. Matter* **2** 281
Watanabe M O and Maeda H 1984 *Japan. J. Appl. Phys.* **23** L734
Watanabe M O, Morizuka K, Mashita M, Ashizawa Y and Zohta Y 1984 *Japan. J. Appl. Phys.* **23** L103